

3-Hydroxyflavones vs. 3-Hydroxyquinolinones: Structure-Activity Relationships and Stability Studies on Ru^{II}(arene) Anticancer Complexes with Biologically Active Ligands

Andrea Kurzwernhart,^{a,b} Wolfgang Kandioller,^{a,b} Éva A. Enyedy,^c Maria Novak,^a Michael A. Jakupec,^{a,b} Bernhard K. Keppler^{a,b} and Christian G. Hartinger^{a,b,d,*}

Ru^{II}(η^6 -arene) complexes, especially with bioactive ligands, are considered as very promising compounds for anticancer drug design. We have shown recently that Ru^{II}(η^6 -*p*-cymene) complexes with 3-hydroxyflavone ligands exhibit very high *in vitro* cytotoxic activities correlating with a strong inhibition of topoisomerase II α . In order to expand the structure-activity relationships and to determine the impact of lipophilicity of the arene ligand and of the hydrolysis rate on anticancer activity, a series of novel 3-hydroxyflavone derived Ru^{II}(η^6 -arene) complexes were synthesised. Furthermore, the impact of the heteroatom in the bioactive ligand backbone was studied by comparing the cytotoxic activity of Ru^{II}(η^6 -*p*-cymene) complexes of 3-hydroxyquinolinone ligands with that of their 3-hydroxyflavone analogues. To better understand the behaviour of these Ru^{II} complexes in aqueous solution, the stability constants and pK_a values for complexes and corresponding ligands were determined. Furthermore, the interaction with the DNA model 5'-GMP and with a series of amino acids was studied in order to elucidate potential biological target structures.

Introduction

Ruthenium complexes represent a promising class of metal-based chemotherapeutics. The octahedral geometry of ruthenium, its binding ability to plasma proteins and the number of possible oxidation states in biological environments, makes it well suitable for drug design.¹ By now, several ruthenium complexes have shown interesting properties *in vivo* and a generally lower toxicity than for platinum drugs was observed.² Two Ru^{III} compounds, namely [ImH][*trans*-Ru(DMSO)(Im)Cl₄] (NAMI-A, Im = imidazole) and [IndH][*trans*-Ru(Ind)₂Cl₄] (KP1019, Ind = indazole) (Chart 1) are currently undergoing clinical trials with very promising results.³⁻⁵

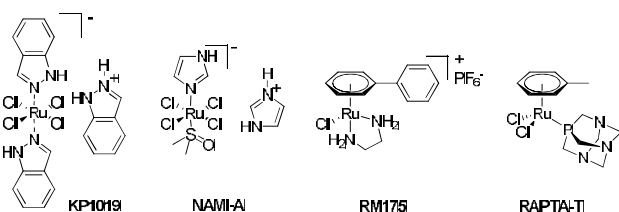


Chart 1. Structures of Ru anticancer agents.

In the course of ruthenium anticancer drug development programmes, organometallic and especially half-sandwich Ru^{II}(η^6 -arene) complexes have more and more demonstrated their potential.⁶⁻¹⁰ Their hydrophobic arene ligand is thought to facilitate the diffusion through the lipophilic cell membrane.¹¹ The three remaining Ru coordination sites can be filled with various mono-, bi- or tridentate ligands, which offers a number of

possibilities to modulate biological and pharmacological properties by proper ligand selection.¹² Important examples for this substance type are Ru^{II}(arene) complexes of bidentate ethylenediamine, such as RM175 (Chart 1), and the RAPTA-type compounds containing the monodentate 1,3,5-triaza-7-phosphatricyclo[3.3.1.1]decane (pta) ligand. RM175 binds to DNA either covalently *via* the N7 of guanine or non-covalently by intercalation of the arene, leading to cell death by modulation of the p53-p21-bax pathway.^{2,13} As opposed to this, the RAPTA compounds have very different chemical and biological properties. RAPTA-T (Chart 1) is selectively activated in the hypoxic conditions of solid tumours and is capable of inhibiting metastasis both *in vitro* and *in vivo*.^{4,14-16} Tethering ethacrynic acid to the arene ligand of RAPTA led to a compound capable of overcoming the glutathione transferase drug resistance mechanism of tumour cells and triggered several biological pathways involving either endonuclease G, caspases or c-Jun N-terminal kinase.¹⁷ This is an example of linking a biological active molecule to a metal centre and modulating thereby its biological properties. Other related approaches involve Ru^{II}(arene) compounds with ligand systems that resemble the kinase inhibitor staurosporine¹⁸ or complexes of paullones, which are cyclin-dependent kinase (CDK) and glycogen synthase kinase-3 inhibitors.¹⁹ More recently, we have demonstrated that Ru^{II}(cym) (cym = η^6 -*p*-cymene) complexes of 3-hydroxyflavones are potent tumour cell growth inhibitors.²⁰

3-Hydroxyflavones belong to the naturally occurring class of flavonoids which are polyphenols of plants, fruits and vegetables. They are well known for their beneficial effects on health due to their antioxidant and antiradical, antiinflammatory, antiviral and anticarcinogenic properties. These effects are caused primarily by

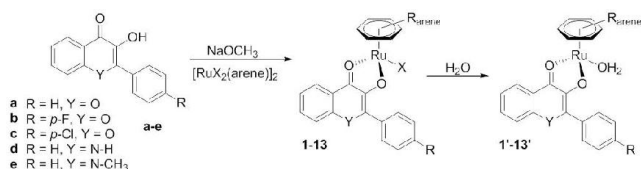
the scavenging of free radicals by the flavonoid structure and by interaction with a number of enzymes.²¹ Flavonoids are capable of forming stable chelate complexes with a broad range of metal ions, which have already shown biological activity in the treatment of diseases like AIDS, diabetes mellitus, some genetic diseases and also cancer.²² The Ru^{II}(cym) complexes of 3-hydroxyflavones were found to exhibit not only high *in vitro* anticancer activity in human cancer cell lines but also inhibit human topoisomerase II α activity, which correlates to their cytotoxic potency.²⁰

In order to study the impact of the nature of the arene and halogenido ligands on the stability and cytotoxic activity, a series of Ru^{II}(arene)X complexes with 3-hydroxyflavones has been synthesised. These properties are compared with those of structurally related 3-hydroxyquinolinone complexes featuring a nitrogen atom in the heterocyclic ligand. These studies are complemented with UV/vis and fluorescence spectroscopy experiments to gain information on the stability and pK_a values of the hydrolysis products and ligand systems.

Results and discussion

Synthesis

Within the course of a project to prepare 3-hydroxy-4-pyrone complexes, we have reported the synthesis of ruthenium(II)-cymene complexes with various substituted 3-hydroxyflavones and the influence of the substitution pattern and the nature of the substituent on the *in vitro* anticancer activity was studied.^{20,23} In order to extend the structure-activity relationships (SARs), a series of Ru^{II}(arene) complexes with 3-hydroxyflavones **a–c** and 3-hydroxyquinolinones **d** and **e** was synthesised by deprotonation of the ligands with sodium methoxide and subsequent reaction with the respective bis[dihalido(η^6 -arene)ruthenium(II)] ([RuX₂(arene)]₂; η^6 -arene = cym, toluene, biphenyl; X = Cl, Br, I), yielding complexes **1–13** in good to very good yields (Scheme 1). The compounds were characterised with standard analytical methods (see experimental part) and were stable for over one year though exposed to sunlight and air.



	ligand	X	R _{arene}		ligand	X	R _{arene}
1 ^a	a	Cl	cym	8	a	Cl	tol
2 ^a	b	Cl	cym	9	c	Cl	tol
3 ^a	c	Cl	cym	10	a	Cl	biphen
4	a	Br	cym	11	c	Cl	biphen
5	c	Br	cym	12	d	Cl	cym
6	a	I	cym	13	e	Cl	cym
7	c	I	cym				

Scheme 1. Synthesis of Ru^{II}(η^6 -arene) complexes **1–13** and formation of the hydrolysis products **1'–13'** in aqueous solution. ^a from refs. 20,23.

Behaviour and stability in aqueous solution

In order to study the properties of the 3-hydroxyflavone-derived Ru^{II}(cym) complexes in aqueous solution, the proton dissociation process of the *p*-fluoro-substituted ligand **b**, the hydrolysis of [Ru^{II}(cym)X₃]ⁿ⁺ (n = -1 - 2; X = Cl⁻, H₂O or DMSO, Supporting Information) and the complex formation process of the

corresponding complex **2** were investigated and stability and dissociation constants were studied.

Proton dissociation process of ligand **b**

The proton dissociation constant (pK_a) of ligand **b** was determined by UV-vis spectrophotometry in 20% (w/w) dimethyl sulfoxide (DMSO)/H₂O because of the poor solubility of the ligand and its complex in pure water. Since flavonoids may suffer from photodegradation,²⁴ spectra were measured at various pH values employing the batch technique instead of continuous titrations. This guarantees minimal UV exposure and helps avoiding photolysis, especially at high pH values (Figure 1). The pH-dependent spectra of the ligand show characteristic changes at increasing pH values. The deprotonation (HL \rightleftharpoons L⁻ + H⁺) attributed to the hydroxyl functional group is accompanied by a bathochromic shift of the λ_{\max} and a small increase in intensity. The isosbestic point is constant at 366 nm up to pH 10.4 but shifts at higher pH most probably due to the photodegradation of the ligand. Therefore, the pK_a value of 8.70 \pm 0.01 and the individual spectra of the ligand species (HL, L⁻; Figure 1b) were calculated on the basis of deconvoluted spectra recorded at pH < 10.4. The λ_{\max} values of both the protonated and the deprotonated forms of ligand **b** are identical to those of the unsubstituted 3-hydroxyflavone **a**.²⁵ However, its pK_a value is significantly lower due to the electron withdrawing effect of the fluoro substituent. The pK_a of the structurally related pyrone ligand maltol (8.76 \pm 0.01), which was also determined under the same conditions, was in the same range as that of **b**.²⁶

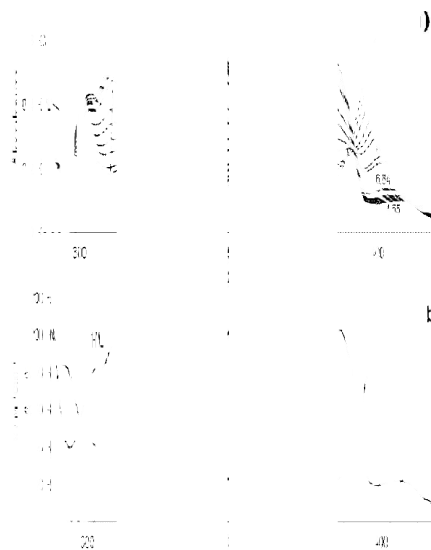


Fig. 1. UV-vis spectra of ligand **b** at various pH values (a) and calculated individual absorbance spectra of the HL and L⁻ species (b) {c_{ligand} = 5 \times 10⁻⁵ M; T = 25°C; I = 0.20 M (KCl); 20% (w/w) DMSO/H₂O}. HL: λ_{\max} = 342 nm ($\lambda_{342\text{ nm}}$ = 10210 mol⁻¹ dm³ cm⁻¹); L⁻: λ_{\max} = 402 nm ($\lambda_{402\text{ nm}}$ = 10755 mol⁻¹ dm³ cm⁻¹).

In addition, the proton dissociation process of **b** in aqueous phase was monitored by fluorimetry (Figure S1a) at much lower concentration. The ligand excitation maximum was found at 342 nm and the emission spectrum represents two maxima at 504 and 411 nm. The appearance of the two emission bands indicates two pathways for deactivation of the excited state. The pH

dependence of the fluorescence emission spectra shows that the emission intensity is strongly sensitive to the pH, and deprotonation results in a significant decrease of the intensity. From the spectral changes in water a pK_a value of 8.30 ± 0.09 was obtained, which verifies the pK_a determined in 20% (w/w) DMSO/H₂O and which is again in the same range as the pK_a of maltol in aqueous solution (8.44).²⁵

Solution equilibria of $[Ru^{II}(cym)X_3]^{n+}$ and complex **2**

In order to understand the behaviour of the flavonoid complex in aqueous solution, the hydrolysis of $[Ru^{II}(cym)X_3]^{n+}$ ($n = -1 - 2$; $X = Cl^-$, H_2O or $DMSO$) needed to be determined under the same conditions. This was studied in 20% (w/w) DMSO/H₂O by UV-vis spectrophotometric titrations (Figure S2). Based on the spectral changes, stability constants of the minor $[Ru_2(cym)_2(OH)_2X_m]^{n+}$ ($m = 1, 2$) and the major $[Ru_2(cym)_2(OH)_3]^+$ dinuclear hydrolysis products were determined as $\log\beta$ $[(Ru(cym))_2H_2]^{2+} = -9.85 \pm 0.06$ and $\log\beta$ $[Ru_2(cym)_2H_3]^+ = -15.11 \pm 0.03$, respectively (Supporting Information). As the titrations were performed in the presence of 0.2 M KCl, these constants are regarded as conditional stability constants. Similar but not identical speciation was found in pure aqueous solution.²⁷ The presence of DMSO can suppress the hydrolysis of $[Ru^{II}(cym)X_3]^{n+}$ which is then shifted to higher pH values (Figure S2b).

The complex formation processes of the ruthenium(II)-cym complex **2** were studied under the same conditions as for $[Ru^{II}(cym)X_3]^{n+}$ (Figure 2a) and is compared to the maltol-ruthenium(II)-cym system (Figure 2b).¹¹ The pH-dependent spectral changes of the ruthenium(II)-cym-containing systems (Figure 2c) compared to the free ligands reveal that the complex formation starts $pH > \sim 4$ in both cases. The complex formation results in a significant shift of the λ_{max} values and this new band is different from the bands belonging to the protonated and deprotonated forms of the metal-free ligands. This band is especially well-separated in the case of **2** (Figure 2a) (*i.e.* λ_{max} of complex: 436 nm, HL: 342 nm, L^- : 402 nm). Analysis of changes in the overlapping ligand and charge transfer (CT) bands shows the exclusive formation of mononuclear species $[Ru^{II}(cym)(L)X]^{n+}$ with a 1:1 metal-to-ligand ratio. By deconvolution of the UV-vis spectra (Figure S3), a stability constant $\log\beta$ ($[Ru^{II}(cym)(L)X]^{n+}$) = 7.13 ± 0.08 for **2** was determined, which is in about the same range as the maltolato complex ($\log\beta = 7.04 \pm 0.05$).

At neutral and alkaline pH various parallel processes take place, namely the complex $[Ru^{II}(cym)(L)X]^{n+}$ starts to hydrolyse forming the mixed hydroxido species $[Ru^{II}(cym)(L)(OH)]$ and to dissociate giving the *tris*-hydroxido-bridged dinuclear species $[Ru_2(cym)_2(OH)_3]^+$ and the metal-free ligand (Figure 2d). The dissociation of (*O,O*)-pyrone ligands such as maltol of *mono*-ligand complexes is relatively slow.²⁸ However, in case of flavonoid complexes, the photodegradation of the ligand is a possible side reaction at $pH > \sim 10$. Due to these reasons the deconvolution of the spectra becomes more difficult and stability data of the $[Ru^{II}(cym)(L)(OH)]$ species could only be obtained with lower accuracy as $\log\beta = 0.3 \pm 0.1$ for **2** and 0.1 ± 0.1 for maltol.

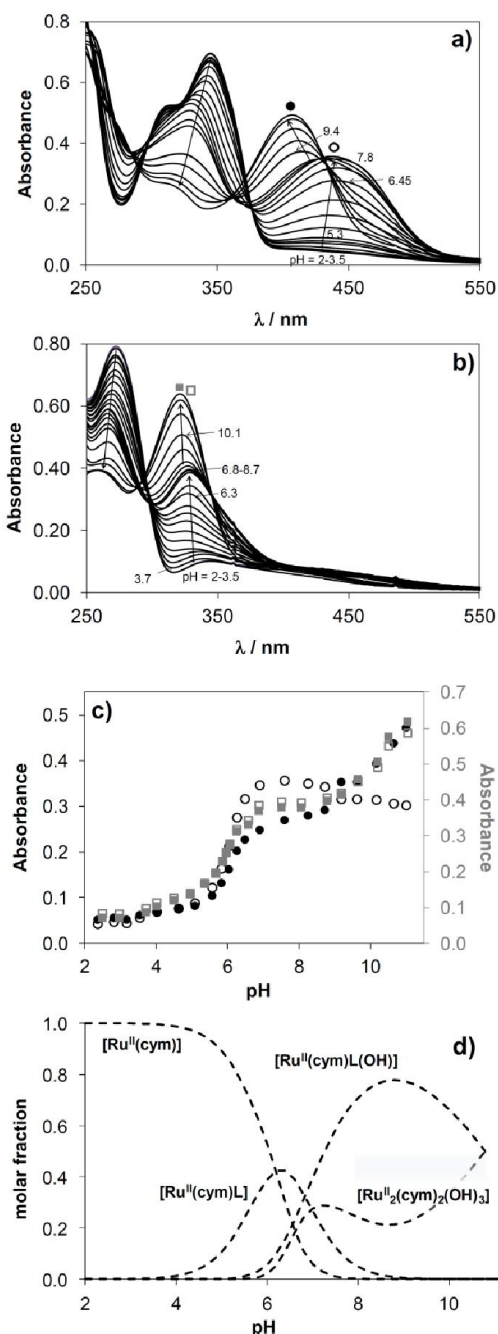


Fig. 2. (a) UV-vis spectra of **2** and (b) for comparison of a maltolato $Ru^{II}(cym)$ complex at various pH values. (c) Absorbance values at 402 nm (\bullet) and at 436 nm (\circ) for complex **2** and at 322 nm (\blacksquare) and at 328 nm (\square) for the maltolato $Ru^{II}(cym)$ complex plotted against the pH value. (d) Concentration distribution curves of the complex **2** ($c_{complex} = 5 \times 10^{-5}$ M (8×10^{-5} M in the case of maltol); $T = 25$ °C; $I = 0.20$ M (KCl); 20% (w/w) DMSO/H₂O; $pH = 2.5-11.5$).

Based on the increased proton dissociation constants of ligand **b** and maltol (see above), higher stability constants of $[Ru^{II}(cym)(L)X]^{n+}$ are expected in 20% (w/w) DMSO/H₂O than in pure aqueous solution. However, a $\log\beta = 9.05$ was reported for the maltolato complex in water,²⁹ which is actually by two orders of magnitude higher than the constant obtained in 20% (w/w) DMSO/H₂O mixture. DMSO complexes of Ru^{II} are known and DMSO coordination can suppress the formation of

[Ru^{II}(cym)(L)X]ⁿ⁺ complexes. The speciation and the stability of **2** and the maltolato complex show very strong similarities due to similar metal binding sites of the ligands. The fluorescence spectra of ligand **b** (Figure S1a) and complex **2** in aqueous solution (Figure S1b) show similar features up to pH ~4. When further increasing the pH, a band with high intensity at 448 nm develops reaching a maximum at pH ~5 and decreasing upon increasing pH. The appearance of this strong new band is most probably related to the formation of [Ru^{II}(cym)(L)X]ⁿ⁺, while the formation of the mixed hydroxido species [Ru^{II}(cym)(L)(OH)] is accompanied by a considerable loss of intensity. Therefore, this latter species seems to be much less fluorescent than [Ru^{II}(cym)(L)X]ⁿ⁺, but somewhat more fluorescent than the metal-free ligand. As also found for the maltolato complex, partial hydrolysis and dissociation of **2** are probable at physiological pH.

Reactivity towards biomolecules

In aqueous solution, compounds **1-3**,²⁰ **5**, **7**, **9** and **11** are aquated immediately to the charged aqua species **1'-3'**, **5'**, **7'**, **9'** and **11'**, which can further react with biomolecules. The solubility of **4**, **6**, **8** and **10** in aqueous solution limited investigations, however, due to the structural similarity similar behavior is expectable. Several Ru^{II}(arene) complexes are known to bind to the DNA model compound 5'-GMP and therefore are also able to form adducts with DNA, which is a possible target for metal-based anticancer agents.^{1,2,11,30-33} Similarly, **5**, **7**, **9** and **11** show interactions with 5'-GMP, as observed in ¹H NMR spectroscopy studies. However, due to their low solubility and even lower solubility of their 5'-GMP adducts, the binding mode and stability of the adducts are elusive.

The 3-hydroxyquinolinone-derived Ru^{II}(arene) complexes **12** (Figure S4) and **13** show the same aquation behaviour, but already 5 min after addition of D₂O the first signs of the hydrolysis side product [Ru₂(η⁶-arene)₂(OH)₃]⁺ were observed in the ¹H NMR spectrum, which increased within 24 h. This side product is thermodynamically stable and unreactive towards nucleophiles.⁷ Compounds **12** and **13** bind immediately to the N7 atom of 5'-GMP as indicated by an upfield shift of the H8 signal of 5'-GMP from approximately δ = 8.1 to 7.6 ppm (Figure S5).

To gain more insight into possible interactions with proteins and pharmacokinetic pathways, the reactions of the representative hydrolysis products **1'**, **12'** and **13'** with the amino acids L-methionine, L-histidine, L-cysteine and glycine were investigated (Figures S6-S12). The reactivity was found to be similar to pyrone-derived Ru^{II}(cym) complexes. All compounds reacted immediately with Met and His by replacement of the aqua ligand with the respective amino acid, which is coordinated to the Ru^{II} centre *via* the sulphur atom or *via* the N1 or N3 atoms of the imidazole moiety, respectively.¹¹ In the case of **1'**, the ligand was cleaved off and precipitated completely within 24 h. The same behaviour was observed for the 3-hydroxyquinolinone-derived complexes. However, after 24 h especially for **12'** still signals of coordinated quinolinone ligands were visible. This may be due to a slightly higher stability of the 3-hydroxyquinolinone complexes towards reaction with amino acids. Addition of Cys led to immediate decomposition of **1'** and to a lower extent of **13'**. For **12'** a reaction with Cys was observed (Figure 3) but the compound also decomposed partly within 24 h. In the case of

glycine, also differing behaviour between 3-hydroxyflavone and quinolinone complexes was observed. Glycine reacted immediately with **1'**, whereas the reaction with **12'** and especially **13'** was significantly slower. Two minutes after addition only traces of coordinated glycine (two doublets at approximately δ = 3.1 ppm)¹¹ were observed in **12'** and only after 18 h in **13'**, indicating again higher stability of the 3-hydroxyquinolinone complexes concerning reactions with amino acids. However, the cytotoxicity of 3-hydroxyflavone and quinolinone Ru^{II}(cym) complexes was similar (see below), although the MTT assay to determine the IC₅₀ values is carried out in amino acid-containing medium. This indicates that the reaction with amino acids does not seem to significantly alter their *in vitro* anticancer potency, most probably due to their higher lipophilicity which may result in enhanced cellular uptake.

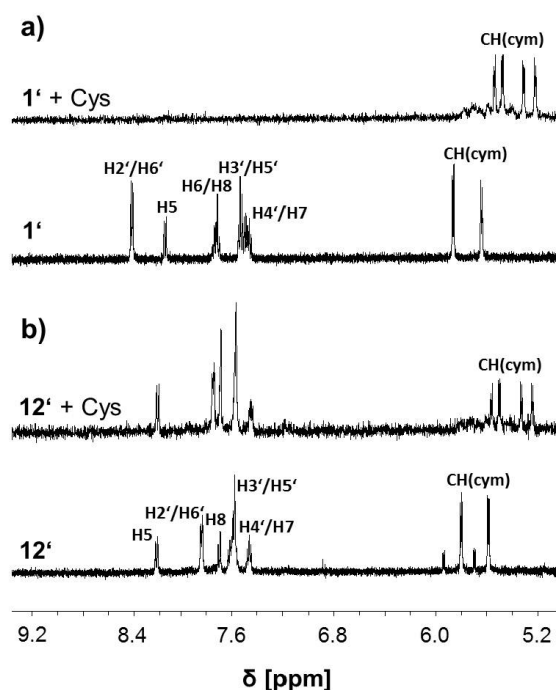


Fig. 3. Reaction mixtures of **1'** (a) and **12'** (b) with equimolar amounts of L-cysteine analysed by ¹H NMR spectroscopy after 5 min show immediate decomposition of **1'** after addition of Cys, whereas minor effects on the quinolinone signals of **12'** were observed.

In vitro anticancer activity

The cytotoxic activity of the Ru^{II}(arene) complexes was determined in the human cancer cell lines CH1 (ovarian carcinoma), SW480 (colon carcinoma) and A549 (non-small cell lung carcinoma) by means of the colorimetric MTT assay (Table 1). Recently, we have shown that the type and especially the position of the substituent on the phenyl ring of the ligand have a crucial impact on their biological activity.²⁰ *Meta*- and *para*-substitution led to more cytotoxic compounds, whereas *ortho*-substituted or unsubstituted ligand structures showed less *in vitro* potency (Table 1, compare compounds **2** and **3** with **1**). These data correlate well with the inhibition of topoisomerase II α activity. All synthesised complexes exhibit promising tumour-inhibiting properties with IC₅₀ values in the low μ M range, which is very remarkable for Ru^{II}(arene) complexes. In order to

determine the effect of the lipophilicity on the anticancer activity, complexes bearing different arene ligands were synthesised. The toluene derivatives **8** and **9** exhibit a similar activity to their Ru^{II}(cym) analogues **1** and **3**, whereas the biphenyl complexes **10** and **11** are slightly less cytotoxic. Therefore, the influence of the arene ligands seems to be of minor importance for this type of compounds. The same activity pattern was observed for pyrone and especially thiopyrone-derived Ru^{II}(arene) complexes,¹⁹ which is in contrast to for example ethylenediamine complexes. The latter compound class showed a strong dependence of cytotoxicity on the coordinated arene. The change from benzene to *p*-cymene to biphenyl resulted in a large increase of their growth inhibitory activity in relation to an increasing size and hydrophobicity.³⁴ It may be that the change in lipophilicity by the modification of the arene ligand is too marginal to outperform the contribution of the flavonoid ligand on the lipophilicity. Furthermore, as already shown for analogous pyrone- and thiopyrone Ru^{II}(arene) derivatives and also for ethylenediamine complexes, different halides as leaving groups show only little or no impact on the antiproliferative activity (compare **1**, **3**, **4–7**). This can be explained by the quick aqation of the Ru centre, leading to the same aqua products.

When changing from 3-hydroxyflavones to 3-hydroxyquinolinones as ligands, no improvement of the *in vitro* anticancer activity was observed. The quinolinone complexes **12** and **13** exhibit cytotoxic activities in the same range as **1**. Also variation of the unsubstituted 3-hydroxyquinolinone **12** to the 1-methylated form in **13** showed no impact on the cytotoxic activity, indicating that the backbone of the ligand rather than the functional group seems to be crucial for the biological activity of this type of Ru^{II}(arene) complexes.

Table 1. *In vitro* anticancer activity of **1–13** in ovarian (CH1), colon (SW480) and non-small cell lung carcinoma (A549) cell lines.^a

	R	Y	X	arene	IC ₅₀ [μM]		
					CH1	SW480	A549
1 ^b	H	O	Cl	cym	2.1 ± 0.2	9.6 ± 1.5	20 ± 2
2 ^b	<i>p</i> -F	O	Cl	cym	1.7 ± 0.4	7.9 ± 2.1	18 ± 1
3 ^b	<i>p</i> -Cl	O	Cl	cym	0.9 ± 0.1	3.8 ± 0.5	9.5 ± 0.5
4	H	O	Br	cym	2.8 ± 0.4	12 ± 1	27 ± 3
5	<i>p</i> -Cl	O	Br	cym	0.9 ± 0.1	3.4 ± 0.4	7.9 ± 0.6
6	H	O	I	cym	1.6 ± 0.2	9.6 ± 1.5	16 ± 1
7	<i>p</i> -Cl	O	I	cym	1.2 ± 0.3	4.7 ± 0.9	8.9 ± 0.8
8	H	O	Cl	tol	3.2 ± 0.1	12 ± 3	19 ± 1
9	<i>p</i> -Cl	O	Cl	tol	0.9 ± 0.2	4.7 ± 0.6	7.8 ± 2.5
10	H	O	Cl	biphen	5.5 ± 1.2	9.2 ± 1.9	28.3 ± 5.0
11	<i>p</i> -Cl	O	Cl	biphen	6.3 ± 1.1	21.1 ± 4.0	59.1 ± 1.1
12	H	N-H	Cl	cym	4.0 ± 0.2	14 ± 1	17 ± 2
13	H	N-CH ₃	Cl	cym	5.3 ± 0.2	12 ± 2	19 ± 1

^a IC₅₀ = 50% inhibitory concentration, 96 h exposure. ^b taken from refs. 20,23. tol = toluene, biphen = biphenyl.

Conclusions

Ru^{II}(arene) complexes bearing biologically active ligand systems exhibit very interesting features and promising properties for anticancer drug design.¹² 3-Hydroxyflavone-derived Ru^{II}(arene) complexes are potent cytotoxic agents with good correlation to their topoisomerase IIa inhibitory activity.²⁶ We have extended the series of compounds by varying the arene and halido ligands

to learn about their influence on the biological activity, as well as compared the 3-hydroxyflavone complexes to quinolinone analogues in terms of cytotoxicity and reactivity towards biomolecules. All compounds exhibit *in vitro* anticancer activity in the low μM range and showed interaction with the DNA model compound 5'-GMP. Substitution of the arene and halido ligands had only a minor effect on the cytotoxic activity. The 3-hydroxyquinolinone analogues behave similarly to the flavones in aqueous solutions and in anticancer activity assays, but are more stable in presence of amino acids. Extensive solution phase studies by NMR, UV-vis and fluorescence spectroscopy revealed that the *para*-fluoro substituted 3-hydroxyflavone **b** [2-(4-fluorophenyl)-3-hydroxy-4H-chromen-4-one] exhibits a proton dissociation constant (pK_a) of 8.70 ± 0.01 in 20% (w/w) DMSO/H₂O and of 8.30 ± 0.09 in aqueous solution. The complex formation processes of the corresponding ruthenium(II)-cym complex **2** starts at pH > ~4, forming mononuclear species [Ru^{II}(cym)(L)X]ⁿ⁺ with a stability constant of logβ = 7.13 ± 0.08. At pH ≥ 7, hydrolysis of [Ru^{II}(cym)(L)X]ⁿ⁺ leads to the mixed hydroxido species [Ru^{II}(cym)(L)(OH)] (logβ = 0.3 ± 0.1) and partial dissociation giving the *tris*-hydroxido-bridged dinuclear species [Ru₂(cym)₂(OH)₃]⁺ and the metal-free ligand. The stability constants of the hydroxyflavone-derived ruthenium(II)-cym compounds are therefore in the range of structurally-related maltolato complexes.

Considering stability data and *in vitro* anticancer activity, 3-hydroxyflavones seem to be a well-suited ligand system for anticancer Ru^{II}(cym)(chlorido) complexes and those represent a promising compound class for further drug design.

This work was supported by the Hungarian Research Foundation OTKA 103905 and É.A. Enyedy gratefully acknowledges the financial support of J. Bolyai research fellowship. We thank the University of Vienna, the Austrian Science Fund (FWF), the Johanna Mahlke geb. Obermann Foundation, and COST D39 for financial support. We gratefully acknowledge Filip Groznica for doing parts of the synthetic work.

Experimental part

Materials and methods

All solvents were dried and distilled prior to use. All chemicals were purchased from commercial suppliers and used without further purification. Bis[(η⁶-*p*-cymene)dichloridoruthenium(II)], bis[dichlorido(η⁶-toluene)ruthenium(II)], bis[(η⁶-biphenyl)dichloridoruthenium(II)], bis[dibromido(η⁶-*p*-cymene)ruthenium(II)], bis[(η⁶-*p*-cymene)diiodidoruthenium(II)], 3-hydroxy-2-phenyl-4H-chromen-4-one (**a**), 2-(4-fluorophenyl)-3-hydroxy-4H-chromen-4-one (**b**), 2-(4-chlorophenyl)-3-hydroxy-4H-chromen-4-one (**c**), [chlorido {3-(oxo-κO)-2-phenyl-chromen-4(1*H*)-onato-κO} (η⁶-*p*-cymene)ruthenium(II)] (**1**), [chlorido {3-(oxo-κO)-2-(4-fluorophenyl)-chromen-4(1*H*)-onato-κO} (η⁶-*p*-cymene)ruthenium(II)] (**2**), [chlorido {3-(oxo-κO)-2-(4-chlorophenyl)-chromen-4(1*H*)-onato-κO} (η⁶-*p*-cymene)ruthenium(II)] (**3**),²³ 3-hydroxy-2-phenyl-1*H*-quinolin-4-one (**d**) and 3-hydroxy-1-methyl-2-phenyl-1*H*-quinolin-4-one (**e**)^{37,38} were synthesised according to literature procedures.

Melting points were determined with a Büchi Melting Point B-540 apparatus. Elemental analyses were carried out with a Perkin Elmer 2400 CHN Elemental Analyser at the Microanalytical Laboratory of the University of Vienna. NMR spectra were recorded at 25 °C using a Bruker FT-NMR spectrometer Avance IIITM 500 MHz. ¹H NMR spectra were measured in CDCl₃ at 500.10 MHz and ¹³C{¹H} NMR spectra at 125.75 MHz. The 2D NMR spectra were recorded in a gradient-enhanced mode.

Synthetic procedures

General complexation procedure:

A solution of [(η^6 -arene)RuX(μ -X)]₂ (η^6 -arene = *p*-cymene, toluene, biphenyl; X = Cl, Br, I) in methanol (20 mL) was added to a solution of the ligand and sodium methoxide in methanol (20 mL). The reaction mixture was stirred at room temperature and under argon atmosphere for 20 h (except for **8** and **10** which were stirred for 6 h and **11** and **12** which were stirred for 5 h). The solvent was evaporated in vacuum; the residue was dissolved in dichloromethane, filtered and concentrated. Pure complexes were obtained by recrystallisation from methanol or precipitation from methanol with diethyl ether.

[Bromido{3-(oxo- κ O)-2-phenyl-chromen-4(1H)-onato- κ O}(η^6 -*p*-cymene)ruthenium(II)] (4): The reaction was performed according to the general complexation procedure using **a** (159 mg, 0.67 mmol), NaOMe (40 mg, 0.73 mmol) and [Ru(η^6 -*p*-cymene)Br₂]₂ (200 mg, 0.25 mmol) affording **4** as an orange powder (130 mg, 47%). Mp: 169–171 °C (decomp.); ¹H NMR (500.10 MHz, CDCl₃): δ = 1.44–1.45 (m, 6H, CH_{3,Cym}), 2.44 (s, 3H, CH_{3,Cym}), 3.02–3.08 (m, 1H, CH_{3,Cym}), 5.40–5.41 (m, 2H, H3/H5_{Cym}), 5.68 (dd, ³J(H,H) = 5 Hz, ³J(H,H) = 5 Hz, 2H, H2/H6_{Cym}), 7.33–7.36 (m, 1H, H7), 7.38–7.41 (m, 1H, H4'), 7.46–7.50 (m, 2H, H3'/H5'), 7.56 (d, ³J(H,H) = 8 Hz, 1H, H8), 7.59–7.63 (m, 1H, H6), 8.22 (dd, ⁴J(H,H) = 1 Hz, ³J(H,H) = 8 Hz, 1H, H5), 8.60 (dd, ⁴J(H,H) = 1 Hz, ³J(H,H) = 8 Hz, 2H, H2'/H6') ppm; ¹³C{¹H} NMR (125.75 MHz, CDCl₃): δ = 18.9 (CH_{3,Cym}), 22.7 (CH_{3,Cym}), 31.3 (CH_{3,Cym}), 78.4 (C3/C5_{Cym}), 81.0 (C2/C6_{Cym}), 95.5 (C4_{Cym}), 99.3 (C1_{Cym}), 117.9 (C8), 120.1 (C8a), 124.1 (C7), 124.6 (C5), 127.3 (C2'/C6'), 127.3 (C2'/C6'), 128.2 (C3'/C5'), 129.3 (C4'), 132.5 (C2), 132.6 (C6), 149.1 (C1'), 153.8 (C4a), 154.8 (C3), 183.5 (C4) ppm; elemental analysis calcd for C₂₅H₂₃BrO₃Ru: C 54.35, H 4.20%; found: C 54.36, H 4.25%.

[Bromido{3-(oxo- κ O)-2-(4-chlorophenyl)-chromen-4(1H)-onato- κ O}(η^6 -*p*-cymene)ruthenium(II)] (5): The reaction was performed according to the general complexation procedure using **c** (191 mg, 0.70 mmol), NaOMe (44 mg, 0.81 mmol) and [Ru(η^6 -*p*-cymene)Br₂]₂ (220 mg, 0.28 mmol) affording **5** as a red powder (210 mg, 64%). Mp: 164–167 °C (decomp.); ¹H NMR (500.10 MHz, CDCl₃): δ = 1.43–1.45 (m, 6H, CH_{3,Cym}), 2.43 (s, 3H, CH_{3,Cym}), 3.00–3.07 (m, 1H, CH_{3,Cym}), 5.41 (dd, ⁴J(H,H) = 1 Hz, ³J(H,H) = 8 Hz, 2H, H3/H5_{Cym}), 5.68 (dd, ³J(H,H) = 5 Hz, ³J(H,H) = 5 Hz, 2H, H2/H6_{Cym}), 7.33–7.36 (m, 1H, H7), 7.44 (d, ³J(H,H) = 9 Hz, 2H, H3'/H5'), 7.54 (d, ³J(H,H) = 8 Hz, 1H, H8), 7.60–7.64 (m, 1H, H6), 8.21 (dd, ⁴J(H,H) = 1 Hz, ³J(H,H) = 8 Hz, 1H, H5), 8.55 (d, ³J(H,H) = 9 Hz, 2H, H2'/H6') ppm; ¹³C{¹H} NMR (125.75 MHz, CDCl₃): δ = 19.1 (CH_{3,Cym}), 22.5 (CH_{3,Cym}),

31.3 (CH_{3,Cym}), 78.4 (C3/C5_{Cym}), 81.0 (C2/C6_{Cym}), 95.9 (C4_{Cym}), 99.3 (C1_{Cym}), 117.8 (C8), 120.0 (C8a), 124.2 (C7), 124.7 (C5), 128.4 (C2'/C6'), 128.5 (C3'/C5'), 131.0 (C4'), 132.8 (C6), 134.9 (C2), 147.9 (C1'), 153.8 (C4a), 154.8 (C3), 183.7 (C4) ppm; elemental analysis calcd for C₂₅H₂₂ClBrO₃Ru·0.25H₂O: C 50.77, H 3.83%; found: C 50.79, H 3.77%.

[Iodido{3-(oxo- κ O)-2-phenyl-chromen-4(1H)-onato- κ O}(η^6 -*p*-cymene)ruthenium(II)] (6): The reaction was performed according to the general complexation procedure using **a** (128 mg, 0.54 mmol), NaOMe (33 mg, 0.61 mmol) and [Ru(η^6 -*p*-cymene)I₂]₂ (208 mg, 0.21 mmol) affording **6** as red crystals (177 mg, 70%). Mp: 131–134 °C (decomp.); ¹H NMR (500.10 MHz, CDCl₃): δ = 1.47–1.48 (m, 6H, CH_{3,Cym}), 2.45 (s, 3H, CH_{3,Cym}), 3.05–3.12 (m, 1H, CH_{3,Cym}), 5.45 (dd, ³J(H,H) = 5 Hz, ³J(H,H) = 5 Hz, 2H, H3/H5_{Cym}), 5.73 (dd, ³J(H,H) = 5 Hz, ³J(H,H) = 5 Hz, 2H, H2/H6_{Cym}), 7.34–7.37 (m, 1H, H7), 7.39–7.42 (m, 1H, H4'), 7.47–7.50 (m, 2H, H3'/H5'), 7.58 (d, ³J(H,H) = 8 Hz, 1H, H8), 7.61–7.64 (m, 1H, H6), 8.20 (dd, ⁴J(H,H) = 1 Hz, ³J(H,H) = 8 Hz, 1H, H5), 8.61 (dd, ⁴J(H,H) = 1 Hz, ³J(H,H) = 8 Hz, 2H, H2'/H6') ppm; ¹³C{¹H} NMR (125.75 MHz, CDCl₃): δ = 18.6 (CH_{3,Cym}), 22.7 (CH_{3,Cym}), 31.9 (CH_{3,Cym}), 77.7 (C3/C5_{Cym}), 80.8 (C2/C6_{Cym}), 95.0 (C4_{Cym}), 99.5 (C1_{Cym}), 117.9 (C8), 120.1 (C8a), 124.1 (C7), 124.6 (C5), 127.2 (C2'/C6'), 128.2 (C3'/C5'), 129.3 (C4'), 132.5 (C2), 132.6 (C6), 149.1 (C1'), 153.9 (C4a), 155.1 (C3), 183.7 (C4) ppm; elemental analysis calcd for C₂₅H₂₃IO₃Ru·0.25H₂O: C 49.72, H 3.92%; found: C 49.61, H 3.68%.

[Iodido{3-(oxo- κ O)-2-(4-chlorophenyl)-chromen-4(1H)-onato- κ O}(η^6 -*p*-cymene)ruthenium(II)] (7): The reaction was performed according to the general complexation procedure using **c** (151 mg, 0.55 mmol), NaOMe (36 mg, 0.67 mmol) and [Ru(η^6 -*p*-cymene)I₂]₂ (217 mg, 0.22 mmol) affording **7** as a deep red powder (190 mg, 68%). Mp: 93–95 °C (decomp.); ¹H NMR (500.10 MHz, CDCl₃): δ = 1.45–1.46 (m, 6H, CH_{3,Cym}), 2.42 (s, 3H, CH_{3,Cym}), 3.03–3.09 (m, 1H, CH_{3,Cym}), 5.44 (dd, ³J(H,H) = 5 Hz, ³J(H,H) = 5 Hz, 2H, H3/H5_{Cym}), 5.72 (dd, ³J(H,H) = 5 Hz, ³J(H,H) = 5 Hz, 2H, H2/H6_{Cym}), 7.33–7.36 (m, 1H, H7), 7.43 (d, ³J(H,H) = 9 Hz, 2H, H3'/H5'), 7.54 (d, ³J(H,H) = 8 Hz, 1H, H8), 7.60–7.63 (m, 1H, H6), 8.18 (dd, ⁴J(H,H) = 1 Hz, ³J(H,H) = 8 Hz, 1H, H5), 8.54 (d, ³J(H,H) = 9 Hz, 2H, H2'/H6') ppm; ¹³C{¹H} NMR (125.75 MHz, CDCl₃): δ = 19.1 (CH_{3,Cym}), 22.6 (CH_{3,Cym}), 31.5 (CH_{3,Cym}), 78.0 (C3/C5_{Cym}), 80.9 (C2/C6_{Cym}), 95.6 (C4_{Cym}), 99.3 (C1_{Cym}), 117.9 (C8), 120.0 (C8a), 124.3 (C7), 124.6 (C5), 128.3 (C2'/C6'), 128.5 (C3'/C5'), 131.0 (C4'), 132.9 (C6), 134.9 (C2), 148.0 (C1'), 153.9 (C4a), 155.0 (C3), 183.8 (C4) ppm; elemental analysis calcd for C₂₅H₂₂ClIO₃Ru·0.25H₂O: C 47.03, H 3.55%; found: C 46.95, H 3.50%.

[Chlorido{3-(oxo- κ O)-2-phenyl-chromen-4(1H)-onato- κ O}(η^6 -toluene)ruthenium(II)] (8): The reaction was performed according to the general complexation procedure using **a** (180 mg, 0.76 mmol), NaOMe (45 mg, 0.84 mmol) and [Ru(η^6 -toluene)Cl₂]₂ (200 mg, 0.38 mmol) affording **8** as an orange powder (148 mg, 42%). Mp: 218–220 °C (decomp.); ¹H NMR (500.10 MHz, CDCl₃): δ = 2.41 (s, 3H, CH_{3,Tol}), 5.39 (dd, ³J(H,H) = 5 Hz, ³J(H,H) = 5 Hz, 2H, H2/H6_{Tol}), 5.61 (dd, ³J(H,H)

= 5 Hz, $^3J(\text{H,H}) = 5$ Hz, 1H, H1_{Tol}), 5.88–5.90 (m, 2H, H3/H5_{Tol}), 7.34–7.36 (m, 1H, H7), 7.39–7.42 (m, 1H, H4'), 7.48–7.51 (m, 2H, H3'/H5'), 7.57 (d, $^3J(\text{H,H}) = 8$ Hz, 1H, H8), 7.61–7.64 (m, 1H, H6), 8.24 (dd, $^4J(\text{H,H}) = 1$ Hz, $^3J(\text{H,H}) = 8$ Hz, 1H, H5), 8.61 (dd, $^4J(\text{H,H}) = 1$ Hz, $^3J(\text{H,H}) = 8$ Hz, 2H, H2'/H6') ppm; $^{13}\text{C}\{^1\text{H}\}$ NMR (125.75 MHz, CDCl₃): $\delta = 19.1$ (CH_{3,Tol}), 29.9 (CH_{Tol}), 75.1 (C1_{Tol}), 76.7 (C2/C6_{Tol}), 85.2 (C3/C5_{Tol}), 98.9 (C4_{Tol}), 117.8 (C8), 119.9 (C8a), 124.2 (C7), 124.6 (C5), 127.4 (C2'/C6'), 128.3 (C3'/C5'), 129.4 (C4'), 132.3 (C2), 132.7 (C6), 149.4 (C1'), 153.9 (C4a), 154.6 (C3), 183.4 (C4) ppm; elemental analysis calcd for C₂₂H₁₇ClO₃Ru·0.5H₂O: C 55.64, H 3.82%; found: C 55.87, H 3.72%.

[Chlorido{3-(oxo- κ O)-2-(4-chlorophenyl)-chromen-4(1H)-onato- κ O}(\eta^6-toluene)ruthenium(II)] (9):

The reaction was performed according to the general complexation procedure using **c** (206 mg, 0.76 mmol), NaOMe (45 mg, 0.84 mmol) and [Ru(η^6 -*p*-cymene)Cl₂]₂ (200 mg, 0.38 mmol) affording **9** as red crystals (281 mg, 74%). Mp: 217–219 °C (decomp.); ^1H NMR (500.10 MHz, CDCl₃): $\delta = 2.40$ (s, 3H, CH_{3,Tol}), 5.39 (dd, $^3J(\text{H,H}) = 5$ Hz, $^3J(\text{H,H}) = 5$ Hz, 1H, H1_{Tol}), 5.88–5.91 (m, 2H, H3/H5_{Tol}), 7.34–7.38 (m, 1H, H7), 7.50 (d, $^3J(\text{H,H}) = 8$ Hz, 2H, H3'/H5'), 7.52–7.54 (m, 1H, H4'), 7.56 (d, $^3J(\text{H,H}) = 8$ Hz, 1H, H8), 7.62–7.65 (m, 1H, H6), 8.24 (dd, $^4J(\text{H,H}) = 1$ Hz, $^3J(\text{H,H}) = 8$ Hz, 1H, H5), 8.56 (d, $^3J(\text{H,H}) = 8$ Hz, 2H, H2'/H6') ppm; $^{13}\text{C}\{^1\text{H}\}$ NMR (125.75 MHz, CDCl₃): $\delta = 19.1$ (CH_{3,Tol}), 29.9 (CH_{Tol}), 75.1 (C1_{Tol}), 76.7 (C2/C6_{Tol}), 85.2 (C3/C5_{Tol}), 98.6 (C4_{Tol}), 117.9 (C8), 120.0 (C8a), 124.3 (C7), 124.7 (C5), 128.6 (C2'/C6'/C3'/C5'), 130.8 (C2), 133.0 (C6), 135.1 (C4'), 148.2 (C1'), 153.9 (C4a), 154.6 (C3), 183.6 (C4); elemental analysis calcd for C₂₂H₁₆Cl₂O₃Ru: C 52.81, H 3.22%; found: C 52.62, H 3.14%.

[Chlorido{3-(oxo- κ O)-2-phenyl-chromen-4(1H)-onato- κ O}(\eta^6-biphenyl)ruthenium(II)] (10):

The reaction was performed according to the general complexation procedure using **a** (170 mg, 0.71 mmol), NaOMe (43 mg, 0.80 mmol) and [Ru(η^6 -biphenyl)Cl₂]₂ (200 mg, 0.31 mmol) affording **10** as a deep red powder (279 mg, 86%). Mp: 203–206 °C (decomp.); ^1H NMR (500.10 MHz, CDCl₃): $\delta = 5.91$ –5.93 (m, 1H, H1_{Biphen}), 5.96–5.97 (m, 2H, H2/H6_{Biphen}), 6.01–6.04 (m, 2H, H3/H5_{Biphen}), 7.32–7.35 (m, 1H, H7), 7.39–7.44 (m, 3H, H3'/H5', H10_{Biphen}), 7.47–7.51 (m, 3H, H4', H9/H11_{Biphen}), 7.55 (d, $^3J(\text{H,H}) = 8$ Hz, 1H, H8), 7.60–7.63 (m, 1H, H6), 7.90 (dd, $^4J(\text{H,H}) = 1$ Hz, $^3J(\text{H,H}) = 8$ Hz, 1H, H8/H12_{Biphen}), 8.16 (dd, $^4J(\text{H,H}) = 1$ Hz, $^3J(\text{H,H}) = 8$ Hz, 1H, H5), 8.47 (dd, $^4J(\text{H,H}) = 1$ Hz, $^3J(\text{H,H}) = 8$ Hz, 2H, H2'/H6') ppm; $^{13}\text{C}\{^1\text{H}\}$ NMR (125.75 MHz, CDCl₃): $\delta = 78.4$ (C2/C6_{Biphen}), 78.8 (C1_{Biphen}), 83.0 (C3/C5_{Biphen}), 96.9 (C4_{Biphen}), 117.8 (C8), 120.0 (C8a), 124.2 (C7), 124.5 (C5), 127.4 (C2'/C6'), 128.2 (C3'/C5'), 128.8 (C9/C11_{Biphen}), 129.1 (C8/C12_{Biphen}), 129.4 (C4'), 129.6 (C10_{Biphen}), 132.1 (C2), 132.7 (C6), 135.2 (C7_{Biphen}), 149.5 (C1'), 153.9 (C4a), 154.4 (C3), 183.3 (C4) ppm; elemental analysis calcd for C₂₇H₁₉ClO₃Ru: C 61.42, H 3.63%; found: C 61.16, H 3.62%.

[Chlorido{3-(oxo- κ O)-2-(4-chlorophenyl)-chromen-4(1H)-onato- κ O}(\eta^6-biphenyl)ruthenium(II)] (11):

The reaction was

performed according to the general complexation procedure using **c** (193 mg, 0.71 mmol), NaOMe (43 mg, 0.80 mmol) and [Ru(η^6 -*p*-cymene)Cl₂]₂ (200 mg, 0.32 mmol) affording **11** as deep red crystals (245 mg, 68%). Mp: 194–197 °C (decomp.); ^1H NMR (500.10 MHz, CDCl₃): $\delta = 5.91$ –5.93 (m, 1H, H1_{Biphen}), 5.95–5.97 (m, 2H, H2/H6_{Biphen}), 6.02–6.05 (m, 2H, H3/H5_{Biphen}), 7.33–7.38 (m, 3H, H3'/H5'/H7), 7.49–7.55 (m, 4H, H6/H8/H9/H11_{Biphen}), 7.60–7.64 (m, 1H, H10_{Biphen}), 7.88–7.90 (m, 1H, H8/H12_{Biphen}), 8.16 (dd, $^4J(\text{H,H}) = 1$ Hz, $^3J(\text{H,H}) = 8$ Hz, 1H, H5), 8.41 (d, $^3J(\text{H,H}) = 9$ Hz, 2H, H2'/H6') ppm; $^{13}\text{C}\{^1\text{H}\}$ NMR (125.75 MHz, CDCl₃): $\delta = 78.3$ (C2/C6_{Biphen}), 78.5 (C1_{Biphen}), 83.0 (C3/C5_{Biphen}), 97.1 (C4_{Biphen}), 117.8 (C8), 120.0 (C8a), 124.3 (C7), 124.6 (C5), 128.4 (C2'/C6'), 128.6 (C3'/C5'), 128.9 (C9/C11_{Biphen}), 129.1 (C8/C12_{Biphen}), 129.7 (C10_{Biphen}), 130.6 (C2), 132.9 (C6), 135.1 (C4', C7_{Biphen}), 148.4 (C1'), 153.9 (C4a), 154.4 (C3), 183.5 (C4); elemental analysis calcd for C₂₇H₁₈Cl₂O₃Ru·H₂O: C 55.87, H 3.47%; found: C 55.86, H 3.17%.

[Chlorido{3-(oxo- κ O)-2-phenyl-quinolon-4(1H)-onato- κ O}(\eta^6-p-cymene)ruthenium(II)] (12):

The reaction was performed according to the general complexation procedure using **d** (172 mg, 0.73 mmol), NaOMe (43 mg, 0.8 mmol) and [Ru(η^6 -*p*-cymene)Cl₂]₂ (200 mg, 0.33 mmol) to afford **12** as an orange powder (195 mg, 59%). Mp: 177–180 °C (decomp.); ^1H NMR (500.10 MHz, CD₃OD): $\delta = 1.41$ (m, 6H, CH_{3,Cym}), 2.37 (s, 3H, CH_{3,Cym}), 2.88–2.96 (m, 1H, CH_{Cym}), 5.57 (d, $^3J(\text{H,H}) = 5$ Hz, 2H, H3/H5_{Cym}), 5.81 (d, $^3J(\text{H,H}) = 6$ Hz, 2H, H2/H6_{Cym}), 7.40–7.44 (m, 1H, H7), 7.55–7.63 (m, 4H, H3'/H4'/H5'/H6'), 7.76 (d, $^3J(\text{H,H}) = 8$ Hz, 1H, H8), 8.07–8.09 (m, 2H, H2'/H6'), 8.30 (dd, $^4J(\text{H,H}) = 1$ Hz, $^3J(\text{H,H}) = 8$ Hz, 1H, H5) ppm; $^{13}\text{C}\{^1\text{H}\}$ NMR (125.75 MHz, CD₃OD): $\delta = 17.2$ (CH_{3,Cym}), 21.3 (CH_{3,Cym}), 31.2 (CH_{Cym}), 77.3 (C3/C5_{Cym}), 79.6 (C2/C6_{Cym}), 95.9 (C4_{Cym}), 98.3 (C1_{Cym}), 117.9 (C8), 120.0 (C8a), 122.4 (C5), 123.4 (C7), 128.2 (C3'/C5'), 129.0 (C2'/C6'), 129.4 (C4'), 129.6 (C6), 132.3 (C2), 135.3 (C4a), 136.3 (C1'), 152.6 (C3), 174.9 (C4) ppm; elemental analysis calcd for C₂₅H₂₄ClNO₂Ru·0.8CH₂Cl₂: C 53.90, H 4.49%, N 2.44%; found: C 54.01, H 4.78%, N 2.27%.

[Chlorido{3-(oxo- κ O)-1-methyl-2-phenyl-quinolon-4(1H)-onato- κ O}(\eta^6-p-cymene)ruthenium(II)] (13):

The reaction was performed according to the general complexation procedure using **e** (180 mg, 0.73 mmol), NaOMe (43 mg, 0.8 mmol) and [Ru(η^6 -*p*-cymene)Cl₂]₂ (200 mg, 0.33 mmol) to afford **13** as an orange powder (157 mg, 46%). Mp: 188–190 °C (decomp.); ^1H NMR (500.10 MHz, CD₃OD): $\delta = 1.31$ –1.33 (m, 6H, CH_{3,Cym}), 2.27 (s, 3H, CH_{3,Cym}), 2.77–2.85 (m, 1H, CH_{Cym}), 3.74 (N-CH₃), 5.45 (d, $^3J(\text{H,H}) = 5$ Hz, 2H, H3/H5_{Cym}), 5.67 (d, $^3J(\text{H,H}) = 6$ Hz, 2H, H2/H6_{Cym}), 7.50–7.53 (m, 3H, H3'/H5'/H7), 7.61–7.66 (m, 3H, H2'/H4'/H6'), 7.72–7.75 (m, 1H, H6), 7.87 (d, $^3J(\text{H,H}) = 8$ Hz, 1H, H8), 8.44 (dd, $^4J(\text{H,H}) = 1$ Hz, $^3J(\text{H,H}) = 8$ Hz, 1H, H5) ppm; $^{13}\text{C}\{^1\text{H}\}$ NMR (125.75 MHz, CD₃OD): $\delta = 17.1$ (CH_{3,Cym}), 21.3 (CH_{3,Cym}), 31.2 (CH_{Cym}), 37.6 (N-CH₃), 77.6 (C3/C5_{Cym}), 79.5 (C2/C6_{Cym}), 96.4 (C4_{Cym}), 97.9 (C1_{Cym}), 116.8 (C8), 120.9 (C8a), 123.3 (C5), 123.5 (C7), 128.5 (C3'/C5'), 129.2 (C2'/C6'), 130.1 (C4'), 130.3 (C6), 132.3 (C2), 136.3 (C1'), 141.8 (C4a), 152.9 (C3), 174.0 (C4) ppm; elemental analysis calcd for C₂₅H₂₄ClNO₂Ru·CH₂Cl₂: C 53.52, H 4.66%,

N 2.31%; found: C 53.48, H 4.52%, N 2.20%.

UV-vis spectrophotometric and spectrofluorimetric measurements

Maltol, KCl, KOH, HCl and dimethyl sulfoxide (DMSO) were purchased from Sigma-Aldrich. Stock solutions of maltol, **b** and **2** were prepared in a 20% (w/w) DMSO/H₂O mixture or in H₂O. The stock solution of [Ru^{II}(cym)X₃]ⁿ⁺ was obtained by dissolving a known amount of [Ru^{II}(cym)Cl₂]₂ in water and the exact concentration (~5 × 10⁻³ M) was determined with pH-potentiometric titrations in aqueous solution at 25.0 ± 0.1 °C at an ionic strength of 0.20 M (KCl) employing literature data for [Ru₂(cym)₂(OH)₂X_m]ⁿ⁺ (m = 1, 2) complexes.²⁹

A Hewlett Packard 8452A diode array spectrophotometer was used to record the UV-vis spectra in the interval 200–800 nm. The path length was 1 cm. The measurements for determination of the protonation constants of the ligands and the overall stability constants of the metal complexes were carried out at 25.0 ± 0.1 °C in a 20% (w/w) DMSO/H₂O mixture and at an ionic strength of 0.20 M. The titrations were performed with carbonate-free KOH solutions of known concentration (0.20 M). The concentrations of the KOH and HCl solutions were determined by pH-potentiometric titrations. An Orion 710A pH-meter equipped with a Metrohm combined electrode (type 6.0234.100) and a Metrohm 665 Dosimat burette were used for the pH-potentiometric measurements. The electrode system was calibrated to the pH = -log[H⁺] scale in DMSO/water solvent mixtures by means of blank titrations (strong acid vs. strong base; HCl vs. KOH), similarly to the method suggested by Irving *et al.* in pure aqueous solutions.²⁵ The average water ionisation constant, pK_w, was determined as 14.30 ± 0.02 at 25.0 °C and I = 0.20 M (KCl), which corresponds well to literature data.³⁹ Protonation and stability constants and the individual spectra of the species were calculated with the computer program PSEQUAD.⁴⁰ β(M_pL_qH_r) is defined for the general equilibrium pM + qL + rH ⇌ [M_pL_qH_r], as β(M_pL_qH_r) = [M_pL_qH_r]/[M]^p[L]^q[H]^r where M denotes [Ru^{II}(cym)X₃]ⁿ⁺ and L the completely deprotonated ligand.

The spectrophotometric titrations were performed on samples containing either ligand **b**, maltol or [Ru^{II}(cym)X₃]ⁿ⁺, [Ru^{II}(cym)X₃]ⁿ⁺ and maltol, or complex **2** in 20% (w/w) DMSO/H₂O. The concentration of ligands was 5–8 × 10⁻⁵ M and the metal-to-ligand ratios were 1:1 and 1:2 in the case of maltol over the pH range 2.0–11.5. Complex **2** was titrated at a concentration of 5 × 10⁻⁵ M and [Ru^{II}(cym)X₃]ⁿ⁺ at 1.8 × 10⁻⁴ M. The pH-dependent fluorescence measurements of **b** and **2** were carried out on a Hitachi-4500 spectrofluorimeter with the excitation at 342 nm in aqueous solution at 25.0 ± 0.1 °C and an ionic strength of 0.20 M (KCl). The emission spectra were recorded in 1 cm quartz cell in the pH range 2.0–11.5 using 10 nm/10 nm slit widths. The samples contained the compounds at 1.5 × 10⁻⁵ M concentration.

Due to the photosensitivity of **b** and **2**, the batch technique was used for recording the UV-vis and fluorimetric spectra instead of continuous titrations and the solutions were kept in the dark.

Hydrolysis, interaction with 5'-GMP and amino acids

Hydrolysis and stability in water were investigated by ¹H NMR

spectroscopy. Due to the lipophilic character of the organometallics, all experiments were performed in 10% (v/v) d₆-DMSO/D₂O solutions. For the interaction with 5'-GMP, the complexes (ca. 0.1 mg/mL) were dissolved in 10% (v/v) d₆-DMSO/D₂O, yielding the corresponding highly reactive aqua species. The aqua complexes were converted *in situ* by addition of 50 μL aliquots of 5'-GMP solution (10 mg/mL) into the respective 5'-GMP adduct and the reaction was monitored by ¹H NMR spectroscopy. To investigate the reactivity towards amino acids, the aqua complexes (ca. 0.1 mg/mL) were treated with equimolar amounts of amino acids and ¹H NMR spectra were recorded after 5 min and 24 h.

Cytotoxicity in cancer cell lines

Cell lines and culture conditions

CH1 cells originate from an ascites sample of a patient with a papillary cystadenocarcinoma of the ovary and were a gift from Lloyd R. Kelland, CRC Centre for Cancer Therapeutics, Institute of Cancer Research, Sutton, UK. SW480 (human adenocarcinoma of the colon) and A549 (human non-small cell lung cancer) cells were provided by Brigitte Marian (Institute of Cancer Research, Department of Medicine I, Medical University of Vienna, Austria). All cell culture reagents were obtained from Sigma-Aldrich Austria. Cells were grown in 75 cm² culture flasks (Iwaki) as adherent monolayer cultures in Minimum Essential Medium (MEM) supplemented with 10% heat inactivated fetal calf serum, 1 mM sodium pyruvate, 4 mM L-glutamine and 1% non-essential amino acids (100x). Cultures were maintained at 37 °C in humidified atmosphere containing 95% air and 5% CO₂.

MTT assay

Cytotoxicity was determined by the colorimetric MTT [3-(4,5-dimethyl-2-thiazolyl)-2,5-diphenyl-2H-tetrazolium bromide, Sigma] microculture assay. For this purpose, cells were harvested from culture flasks by trypsinisation and seeded in 100 μL/well aliquots into 96-well microculture plates (Iwaki). Cell densities of 1.5 × 10³ cells/well (CH1), 2.5 × 10³ cells/well (SW480) and 4 × 10³ cells/well (A549) were chosen in order to ensure exponential growth of untreated controls throughout the experiment. Cells were allowed to settle and resume exponential growth in drug-free complete culture medium for 24 h. Stock solutions of the test compounds in DMSO were diluted in complete culture medium so that the maximum DMSO content did not exceed 1%. These dilutions were added in 100 μL/well aliquots to the microcultures and cells were exposed to the test compounds for 96 h. At the end of exposure, all media were replaced by 100 μL/well RPMI1640 culture medium (supplemented with 10% heat-inactivated fetal bovine serum) plus 20 μL/well MTT solution in phosphate-buffered saline (5 mg/ml). After incubation for 4 h, the supernatants were removed, and the formazan crystals formed by viable cells were dissolved in 150 μL DMSO per well. Optical densities at 550 nm were measured with a microplate reader (Tecan Spectra Classic), using a reference wavelength of 690 nm to correct for unspecific absorption. The quantity of viable cells was expressed in terms of T/C values by comparison to untreated controls, and 50% inhibitory concentrations (IC₅₀) were calculated from concentration-effect curves by interpolation. Evaluation is based on means from at least three independent

experiments, each comprising at least three replicates per concentration level.

Notes and references

^a Institute of Inorganic Chemistry, University of Vienna, Waehringer Str. 42, 1090 Vienna, Austria.

^b Research Platform "Translational Cancer Therapy Research", University of Vienna, Waehringer Str. 42, 1090 Vienna, Austria

^c Department of Inorganic and Analytical Chemistry, University of Szeged, Dóm tér 7. H-6720 Szeged, Hungary.

^d The University of Auckland, School of Chemical Sciences, Private Bag 92019, Auckland 1142, New Zealand; Tel: +64 9 373 7955 ext 83220; E-mail: c.hartinger@auckland.ac.nz;

<http://hartinger.wordpress.fos.auckland.ac.nz/>

† Electronic Supplementary Information (ESI) available: The SI contains fluorescence spectra of ligand **b** and complex **2** in aqueous solution, measured and calculated UV-vis absorbance spectra and concentration distribution curves of the Ru^{II}(cym)/ligand **b** system, NMR studies on the stability of **12** in aqueous solution, NMR spectra demonstrating the binding ability of **12'** to the DNA model 5'-GMP and NMR spectra showing the reactions of **1'**, **12'** and **13'** with amino acids. See DOI: 10.1039/b000000x/

1. M. J. Clarke, F. C. Zhu and D. R. Frasca, *Chem. Rev.*, 1999, **99**, 2511-2533.
2. A. Bergamo, C. Gaiddon, J. H. M. Schellens, J. H. Beijnen and G. Sava, *J. Inorg. Biochem.*, 2012, **106**, 90-99.
3. J. M. Rademaker-Lakhai, D. Van Den Bongard, D. Pluim, J. H. Beijnen and J. H. M. Schellens, *Clin. Cancer Res.*, 2004, **10**, 3717-3727.
4. C. G. Hartinger, S. Zorbas-Seifried, M. A. Jakupec, B. Kynast, H. Zorbas and B. K. Keppler, *J. Inorg. Biochem.*, 2006, **100**, 891-904.
5. C. G. Hartinger, M. A. Jakupec, S. Zorbas-Seifried, M. Groessl, A. Egger, W. Berger, H. Zorbas, P. J. Dyson and B. K. Keppler, *Chem. Biodiversity*, 2008, **5**, 2140-2155.
6. P. J. Dyson, *Chimia*, 2007, **61**, 698-703.
7. A. F. A. Peacock and P. J. Sadler, *Chem. Asian J.*, 2008, **3**, 1890-1899.
8. C. G. Hartinger and P. J. Dyson, *Chem. Soc. Rev.*, 2009, **38**, 391-401.
9. G. Gasser, I. Ott and N. Metzler-Nolte, *J. Med. Chem.*, 2011, **54**, 3-25.
10. C. G. Hartinger, N. Metzler-Nolte and P. J. Dyson, *Organometallics*, 2012, **31**, 5677-5685.
11. W. Kandioller, C. G. Hartinger, A. A. Nazarov, C. Bartel, M. Skocic, M. A. Jakupec, V. B. Arion and B. K. Keppler, *Chem. Eur. J.*, 2009, **15**, 12283-12291.
12. G. S. Smith and B. Therrien, *Dalton Trans.*, 2011, **40**, 10793-10800.
13. R. L. Hayward, Q. C. Schornagel, R. Tente, J. C. Macpherson, R. E. Aird, S. Guichard, A. Habtemariam, P. Sadler and D. I. Jodrell, *Cancer Chemother. Pharmacol.*, 2005, **55**, 577-583.
14. C. S. Allardyce, P. J. Dyson, D. J. Ellis and S. L. Heath, *Chem. Commun.*, 2001, 1396-1397.
15. A. Bergamo, A. Masi, P. J. Dyson and G. Sava, *Int. J. Oncol.*, 2008, **33**, 1281-1289.
16. S. Chatterjee, S. Kundu, A. Bhattacharyya, C. G. Hartinger and P. J. Dyson, *J. Biol. Inorg. Chem.*, 2008, **13**, 1149-1155.
17. S. Chatterjee, I. Biondi, P. J. Dyson and A. Bhattacharyya, *J. Biol. Inorg. Chem.*, 2011, **16**, 715-724.
18. E. Meggers, G. E. Atilla-Gokcumen, K. Grundler, C. Frias and A. Prokop, *Dalton Trans.*, 2009, 10882-10888.
19. W. F. Schmid, R. O. John, V. B. Arion, M. A. Jakupec and B. K. Keppler, *Organometallics*, 2007, **26**, 6643-6652.
20. A. Kurzwernhart, W. Kandioller, C. Bartel, S. Bachler, R. Trondl, G. Muhlgaessner, M. A. Jakupec, V. B. Arion, D. Marko, B. K. Keppler and C. G. Hartinger, *Chem. Commun.*, 2012, **48**, 4839-4841.
21. R. J. Nijveldt, E. van Nood, D. E. van Hoorn, P. G. Boelens, K. van Norren and P. A. van Leeuwen, *Am. J. Clin. Nutr.*, 2001, **74**, 418-425.
22. M. Grazul and E. Budzisz, *Coord. Chem. Rev.*, 2009, **253**, 2588-2598.
23. A. Kurzwernhart, W. Kandioller, S. Bächler, C. Bartel, S. Martic, M. Buczkowska, G. Muhlgaessner, M. A. Jakupec, H.-B. Kraatz, P. J. Bednarski, V. B. Arion, D. Marko, B. K. Keppler and C. G. Hartinger, *unpublished data*.
24. S. Tommasini, M. L. Calabro, P. Donato, D. Raneri, G. Guglielmo, P. Ficarra and R. Ficarra, *J. Pharm. Biomed. Anal.*, 2004, **35**, 389-397.
25. O. S. Wolfbeis, A. Knierzinger and R. Schipfer, *J Photochem*, 1983, **21**, 67-79.
26. E. A. Enyedy, L. Horvath, K. Gajda-Schranz, G. Galbacs and T. Kiss, *J. Inorg. Biochem.*, 2006, **100**, 1936-1945.
27. P. Buglyo and E. Farkas, *Dalton Trans.*, 2009, 8063-8070.
28. E. A. Enyedy, E. Sija, T. Jakusch, C. G. Hartinger, B. K. Keppler and T. Kiss, *unpublished data*.
29. L. Biro, E. Farkas and P. Buglyo, *Dalton Trans.*, 2010, **39**, 10272-10278.
30. J. Reedijk, *Chem. Rev.*, 1999, **99**, 2499-2510.
31. H. Chen, J. A. Parkinson, S. Parsons, R. A. Coxall, R. O. Gould and P. J. Sadler, *J. Am. Chem. Soc.*, 2002, **124**, 3064-3082.
32. M. Hanif, H. Henke, S. M. Meier, S. Martic, M. Labib, W. Kandioller, M. A. Jakupec, V. B. Arion, H. B. Kraatz, B. K. Keppler and C. G. Hartinger, *Inorg. Chem.*, 2010, **49**, 7953-7963.
33. M. Hanif, P. Schaaf, W. Kandioller, M. Hejl, M. A. Jakupec, A. Roller, B. K. Keppler and C. G. Hartinger, *Aust. J. Chem.*, 2010, **63**, 1521-1528.
34. R. E. Aird, J. Cummings, A. A. Ritchie, M. Muir, R. E. Morris, H. Chen, P. J. Sadler and D. I. Jodrell, *Br. J. Cancer*, 2002, **86**, 1652-1657.
35. M. A. Bennett and A. K. Smith, *J. Chem. Soc., Dalton Trans.*, 1974, 233-241.
36. M. G. Mendoza-Ferri, C. G. Hartinger, A. A. Nazarov, R. E. Eichinger, M. A. Jakupec, K. Severin and B. K. Keppler, *Organometallics*, 2009, **28**, 6260-6265.
37. H. M. Irving, M. G. Miles and L. D. Pettit, *Anal. Chim. Acta*, 1967, **38**, 475-488.
38. P. Hradil, J. Hlavac and K. Lemr, *J. Heterocycl. Chem.*, 1999, **36**, 141-144.
39. *SCQuery, The IUPAC Stability Constants Database, Academic Software (Version 5.5)*, Royal Society of Chemistry, Sourby Old Farm, Timble, Otley, Yorks, 1993-2005.

40. L. Zékány and I. Nagypál, in *Computational Methods for the Determination of Stability Constants*, ed. D. L. Leggett, Plenum Press, New York, 1985, p. 291.